This is the Pre-Published Version.
C. Xiong, Y. Liu, C. Xu, X. Huang (2021) *Acoustical Extinction of Flame on Moving Firebrand for Fire Protection in Wildland-Urban Interface*, **Fire Technology**. https://doi.org/10.1007/s10694-020-01059-w
This is a post-peer-review, pre-copyedit version of an article published in Fire Technology. The final authenticated version is available online at: https://doi.org/10.1007/s10694-020-01059-w.

Acoustical Extinction of Flame on Moving Firebrand for Fire Protection in Wildland-Urban Interface

Caiyi Xiong[a,b], Yanhui Liu[a], Cangsu Xu[a,c,*] and Xinyan Huang[a,*]

[a]*Department of Building Services Engineering, Hong Kong Polytechnic University, Hong Kong*

[b]*The Hong Kong Polytechnic University Shenzhen Research Institute, Shenzhen 518057, China.*

[c]*College of Energy Engineering, Zhejiang University, Hangzhou, China*

*Correspond to xy.huang@polyu.edu.hk, xucangsu@zju.edu.cn

Abstract

Firebrand is a widely observed phenomenon in wildland fires, which can transport for a long distance, cause spot ignition in the wildland-urban interface (WUI) and increase the rate of wildfire spread. The flame attached to a moving firebrand behaves as the potential pilot source for ignition, so extinguishing such a flame in the process of moving can effectively minimize its fire hazard. In this work, the firebrand used the dry wood ball with a diameter of 20 mm and a weight of 2.9 g, which carried a flame with the heat release rate of 250 W. The firebrand was held by a pendulum system to adjust the velocity. Results showed that there is a minimum sound pressure to extinguish the firebrand flame, which increases slightly with the sound frequency. As the firebrand velocity increases from 0 to 4.2 m/s, the minimum sound pressure for extinction decreases significantly from 114 dB to 90 dB. The cumulative effect of firebrand motion and acoustic oscillation was found to facilitate flame extinction. A characteristic Damköhler number (~1), with the ratio of the fuel residence time to the flame chemical time, is used to quantify the extinction limit of the flaming firebrand. This work provides a technical solution to mitigate the hazard of firebrand flame and spotting ignition in WUI and helps understand the influence of acoustic waves on the flame stability on the solid fuel.

Keywords: sound wave; fire protection; WUI fire; ember; wildfire; extinction

1. Introduction

Controlling flame behavior is an emerging topic in combustion research, where the seeking of improved tactics and technologies for flame suppression and extinction is of particular interest. One promising solution is the use of acoustic waves. It is well known that flame is susceptive to acoustic excitation [1], and the flame response behavior varies with the frequency adopted [2–4]. Many studies focus on reducing the impact of acoustic waves on the flame to improve flame stability, particularly in engine applications, but few studies have tried to use acoustic waves to extinguish the flame.

The U.S. Defense Advanced Research Projects Agency (DARPA) [5] first confirmed the acoustic wave as an effective flame extinguisher, especially in the low-frequency region varying from 35-150 Hz, combined with the sound pressure level (SPL) from 80-150 dB (i.e., 0.2-632 Pa). It also suggested that the critical sound condition for flame extinction was independent of the burner or flame size. Friedman and Stoliarov [6] made attempts in using the low-frequency sound of 30-150 Hz to extinguish the flame on liquid fuels. They found a positive correlation between the extinction pressure and frequency and proposed the extinction as a result of the acoustical disruption of the fuel-flame-supply cycle. For the gas burner flame, Niegodajew *et al.* [7] studied its extinction process using the sound with the frequency of 30-50 Hz and pressure of 128-133 dB (50-89 Pa), and defined a critical acoustic

extinction pressure that is independent of the distance between the flame and sound source. Yamazaki *et al.* [8] found a strong deformation of the non-premixed flame sheet under a sound frequency of 400 Hz. In our previous work [9], the acoustic wave was found to be more effective in extinguishing the fast-moving dripping flame of molten polyethylene than the stationary candle flame. So far, limited research has studied the acoustic extinction of the flame on a moving solid fuel and the associated fire-suppression technology.

Fig. 1. (a) Typical wildland-urban interface (WUI) fire (Source: Denver Post), and (b) firefighting against wildfire and firebrand shower (Source: Australian Federal Police).

With the increasing wildland-urban interface (WUI) fires [10–19] (Fig. 1a), the flying firebrands (or embers) and the associated spotting ignition play significant roles in the fast spread of wildfire [20, 21]. In a wildfire, burning barks and twigs can often detach from the parent fuel due to the drag forces by airflow and be lifted by the fire-induced buoyancy [10, 18, 22]. Many firebrands can fly for miles in the wind and create a firebrand shower [16], which is extremely difficult to track and extinguish (Fig. 1b). In particular, some firebrand particles can carry a flame or transition from smoldering to flaming during the transport and landing processes, which show a significant fire hazard in igniting the WUI combustibles [17, 19, 23]. However, conventional fire suppression technologies cannot handle the flying and flaming firebrand due to the fast and random motion, not to mention the intense firebrand shower with high-density small embers [14–16]. Therefore, more effective firefighting tactics are expected to extinguish the flaming firebrand shower on a large scale. Inspired by the successful acoustic suppression of dripping flame [9], it is hypothesized that the acoustic wave could also be effective in extinguishing the flame on the moving firebrand.

In this experimental work, the well-controlled acoustic wave was applied to extinguish the flame supported by a spherical firebrand with the moving velocity up to 4.2 m/s, and the critical sound regimes for acoustic extinction were quantified under various firebrand transport velocities. Through analyzing the cumulative effect of firebrand motion and acoustic oscillation on the fuel gas and flame, the underlying acoustic extinction mechanism was discussed.

2. Experimental method

A schematic of the experiment setup is illustrated in Fig. 2a, where a Cartesian coordinate (x, y, z) is used to show the geometric position. The system was an upgrade of our previous one [9], which mainly includes a moving spherical firebrand, held by a pendulum system, and an acoustic wave generating system with a speaker, wave generator, and power amplifier.

2.1. Firebrand and flame

Based on the observation in WUI fire scenes [10, 18, 24, 25], a spherical (Schima Superba) hardwood ball with an average diameter of 20 mm was chosen as the representative firebrand, as shown in Fig. 2b. To minimize the influence of fuel moisture content, all samples were first dried in a hot oven with 90 °C for 10 h and then rested inside a temperature and humidity chamber. By doing so, the target balls performed a uniform initial mass of 2.85 ± 0.05 g and moisture content of 2.8 ± 0.2 wt.%. The sample size and its moisture content all follow the range in recent firebrand studies [25–27].

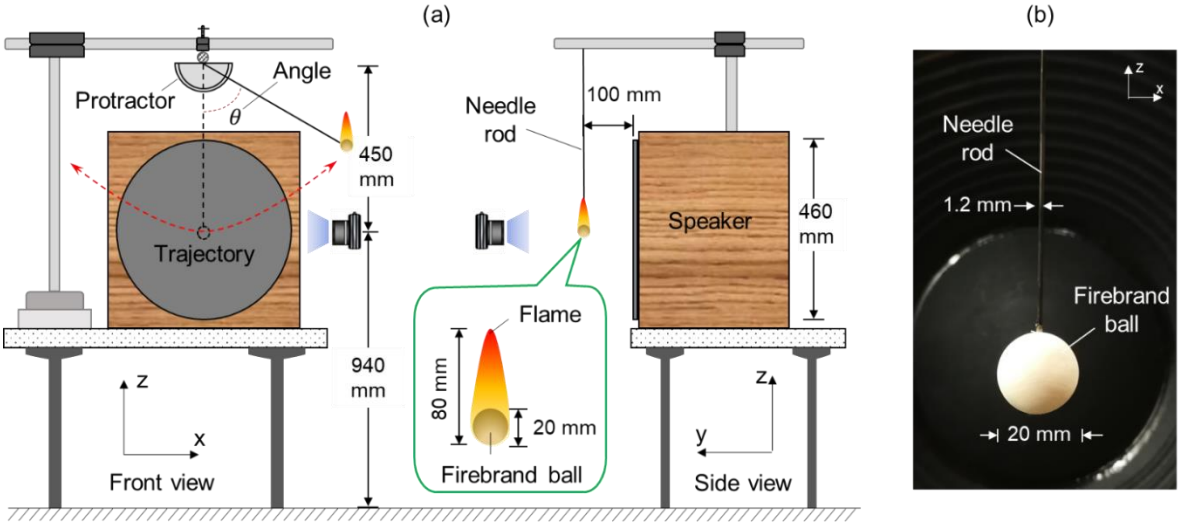

Fig. 2. (a) Schematic of the test setup (front and side views), and (b) spherical wood firebrand.

The target firebrand was initially ignited by a propanol blowtorch when it remains stationary in front of an inactivated speaker. For consistency, the ignition process lasted for 20 s in all tests. After removing the ignitor, the burning of the firebrand ball would develop until the entire ball was covered by the flame (i.e., the envelope flame) with a height of about 80 mm. Fig. 3a shows the evolution of the flame power or the heat release rate (HRR), that is, the product of the measured firebrand mass-loss rates in three repeating tests and a constant heat value of wood (15.8 MJ/kg). A stable burning process with a constant power of 250 ± 20 W occurs around 45 s after ignition and lasts for another 60 s before decaying. In this way, the burning process of the firebrand is well controlled and repeatable.

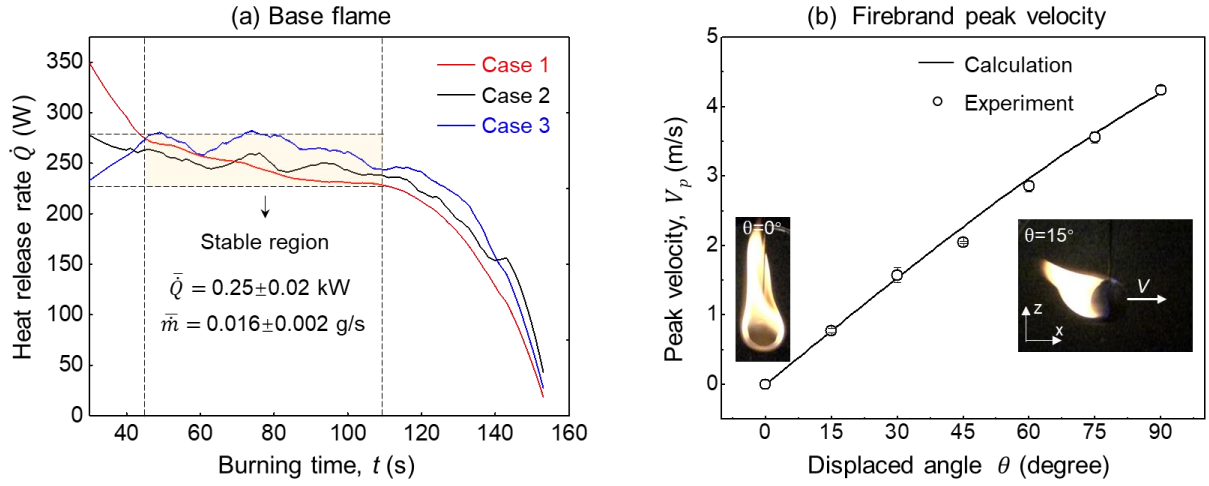

Fig. 3. (a) Time traces of the firebrand HRR in three different trials, and (b) the averaged peak swing velocities (V_p) at different displaced angles (θ).

A pendulum system was employed to achieve the movement of the firebrand (Fig. 2a). The reason for using a pendulum rather than the wind tunnel, because the wind tunnel can product strong background noise to interfere with the main acoustic field. Stainless steel (SS) needle with a length of 450 mm and a diameter of 1.2 mm, whose apex was suspended from a pivot, was inserted to the center of the firebrand ball, and the resting position of the ball coincides with the center axis of speaker. The swing trajectory was restricted in angular direction (x-z plane) and paralleled to and 100-mm in front of the speaker (Fig. 2b). By displacing the needle away from the equilibrium position with a displaced angle (θ), a swing velocity V that shows a peak at the lowest point could be controlled and varied.

Note that the displaced angle here is measured by a protractor fixed at the stationary point of the SS needle (see Fig. 2a), so the vertical and horizontal directions are denoted by θ = 0° and 90°, respectively. Fig. 3b shows the dependence of the peak swing speed (V_p) versus θ, which agrees well with the theoretical curve. The maximum firebrand velocity in this experiment was 4.2 m/s when displacing the needle with θ = 90°, which resides within the range of firebrand in literature [10]. Note that the mass of the SS needle is far higher than that of the firebrand, which drives the pendulum motion.

2.2. Sound source

Since the flame behavior is most sensitive to the low-frequency sound [5–9], a circular bass speaker was used to emit the waves (Fig. 2a). The diameter of the speaker was 460 mm, with the maximum power limit of 800 W. Such a large speaker allowed different firebrands to experience at least one complete acoustic cycle. The acoustic signal was produced by a wave generator, with the wave amplitude defined by a power amplifier. Preliminary tests showed that for this setup, a stationary firebrand flame was sensitive to sound frequency of about 100 Hz. As the frequency increased higher than 105 Hz, the greater sound pressure was also required for flame extinction, which would exceed the power limit of the amplifier. Further, the firebrand flame was reluctant to respond to the sound with a frequency lower than 95 Hz, and the sensitivity depended on the size and shape of the speaker [9]. As such, the target frequency ranged from 95 to 105 Hz was explored in detail.

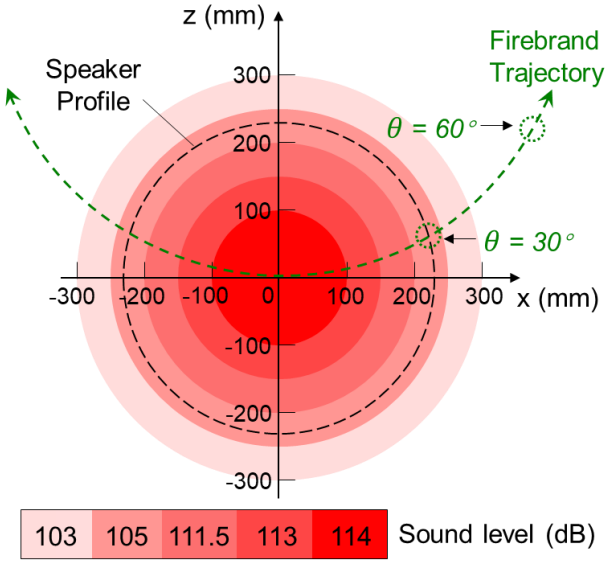

Fig. 4. Sound pressure distribution on the plane of firebrand motion that is 100-mm away from the speaker, where the firebrand trajectory is also shown.

To ensure a uniform acoustic field, the speaker was placed 940 mm above the floor. Also, there was no sidewall nearby for wave reflection. Measurement of the sound level was implemented by a portable

decibel meter after every trial at the flame position, which functioned in the range from 30 to 130 dB with an accuracy of 0.1 dB. Fig. 4 shows the distribution of SPL on a plane of firebrand motion when using a 100 Hz sound at 114 dB. As expected, a semi-uniform sound existed within the range of 100 mm from the speaker center. Given an SPL, if the flame was not extinguished, the SPL would be increased step by step until the extinction occurred. During the experiment, the flame behaviors were monitored by two high-speed cameras (up to 960 fps) from both the front and side views. All experiments were repeated at least three times to minimize the random uncertainty.

3. Results and discussions

Considering a pendulum system was used the exert impetus over firebrand, the firebrand should experience the various speed as time goes by. Therefore, a high criterion was set for the flame extinction, i.e., only if the extinction occurs inside the uniform sound region (or the main acoustic field seen in Fig. 4) and within the initial three swing motions, it is considered as a successful extinction, where the deviation of firebrand velocity from the peak velocity is less than 0.05 m/s. Similar to previous extinguishing experiment on the candle flame [9], given a sound wave, the outcome (extinction or burning) was fixed, so there was no issue of extinction probability. A re-ignition test was conducted for all extinguished firebrand, i.e., check if the target firebrand can be re-ignited by the propanol blowtorch within 2 s, which excludes the possibility of burnout or self-extinction.

3.1. Flame extinction of the stationary firebrand (base case)

Without the activation of the pendulum ($\theta = 0°$), the wood flame should stay statically in front of the speaker, which provides a base case for exploring the critical acoustic condition for flame extinction (see Video A1 in Appendix). Fig. 5 shows a typical extinction process of a stationary flaming firebrand subjected to a 100 Hz sound at 114 dB from the side-view camera (see Video A2 in Appendix).

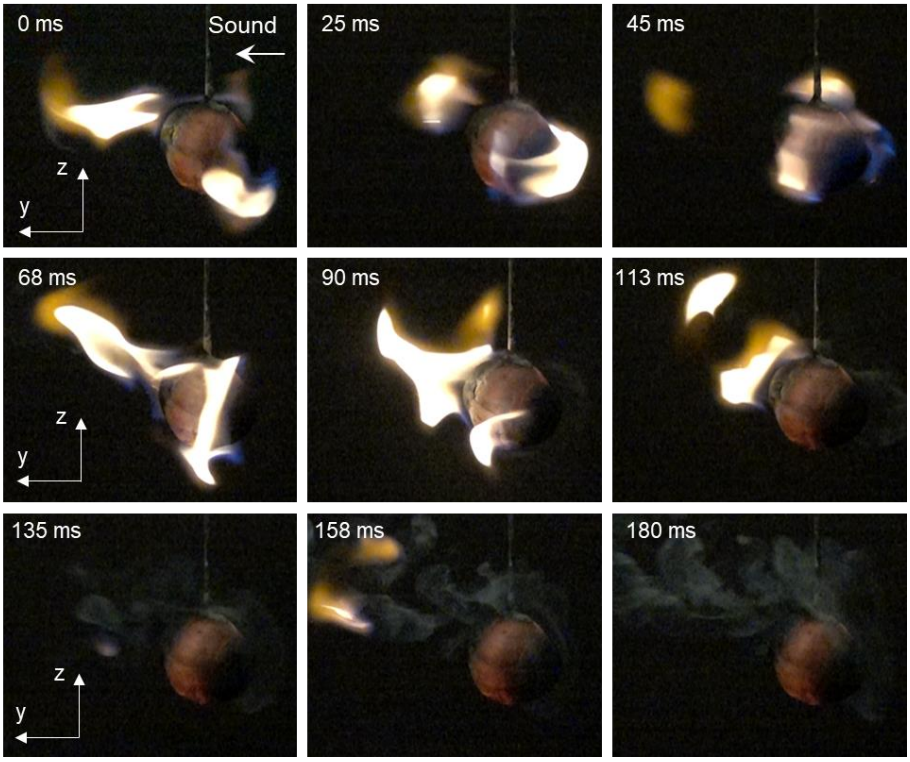

Fig. 5. The extinction process of a stationary firebrand flame in front of the speaker center, recorded by the high-speed camera (960 fps) from side view (Video A2), where the speaker is on the right-hand side, and the time zero is the moment that speaker turns on.

Near extinction, the flame was influenced by the sound wave and shake back and forth around the parent fuel along the direction of sound propagation (y-direction in Fig. 2a). Right before extinction (Δt = 120 ms), the flame appears fully detached from the firebrand, becomes weak rapidly, and creates a large gap between the flame and firebrand. All experiment videos showed that the extinction only occurred when the flame was deflected away from firebrand, where not only the flame heat flux to fuel is significantly reduced, but the flame also cannot reach the pyrolysis gases near the fuel surface. Therefore, this acoustic extinction could be attributed to the reduction of flame heating and pyrolysis gaseous fuel (or the breakage of fuel-flame supply cycle) [7], similar to the extinction of gas-burner and liquid-fuel flames [6].

The critical condition of acoustic extinction at a specified frequency was determined by finding the lowest sound power to cause an immediate extinction within the semi-uniform acoustic field when activating the speaker and repeating 3 times. As seen in Fig. 6, there is a positive correlation between the extinction pressure and frequency, which follows the law of other stationery cases reported in the literature. Compared with extinguishing small candle flame and dripping flame [9], flame extinction on stationary firebrand requires a higher SPL because of a larger burning rate and flame power (or HRR).

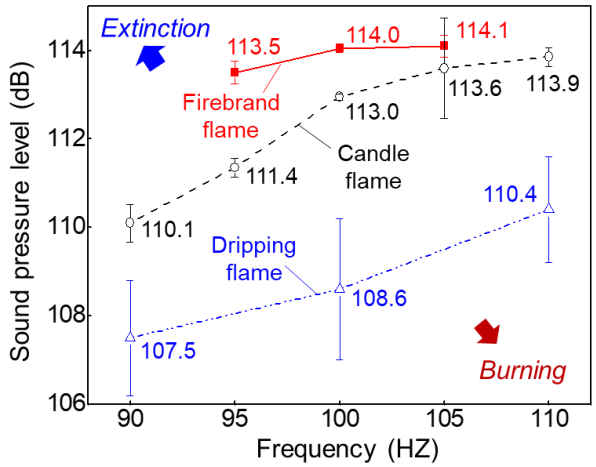

Fig. 6. Correlation between the critical sound pressure and frequency for extinguishing different flames.

3.2. Flame extinction of the moving firebrand

Fig. 7a shows the flame behavior when the firebrand swings with a displaced angle of θ = 60° without using any acoustics (see Video A3 in Appendix), and the camera was placed in front of the speaker (y-direction). Compared with the stationary case, the flame stayed in the wave region and followed the moving firebrand, so only half of the sphere was surrounded by the flame. Also, the flame length was reduced due to the decrease of fuel amount as the convective cooling effect increases. Although the flame would still shake around the moving firebrand, there was no flame extinction observed in this case, nor did the extinction occur in the fastest case when θ = 90°, which excluded the possibility of blowoff, especially when the pendulum changes direction.

After turning on the speaker, enhanced flickering and discontinuous structures were observed with the fluctuations propagating along the flame surface (see Fig. 7b and Video A4 in Appendix). When the sound level reached a specific value, a typical extinction process of the flaming firebrand occurred (see Video A5 in Appendix). Before extinction, the flame became so weak that it was difficult to observe (see Fig. 7c). The distance between the flame base and firebrand here seems not as big as that in the stationary condition (Fig. 5). This is caused by the position and view of the camera, that is, the moving flame detaches in both x and y directions, while the stationary flame only detaches in the x direction.

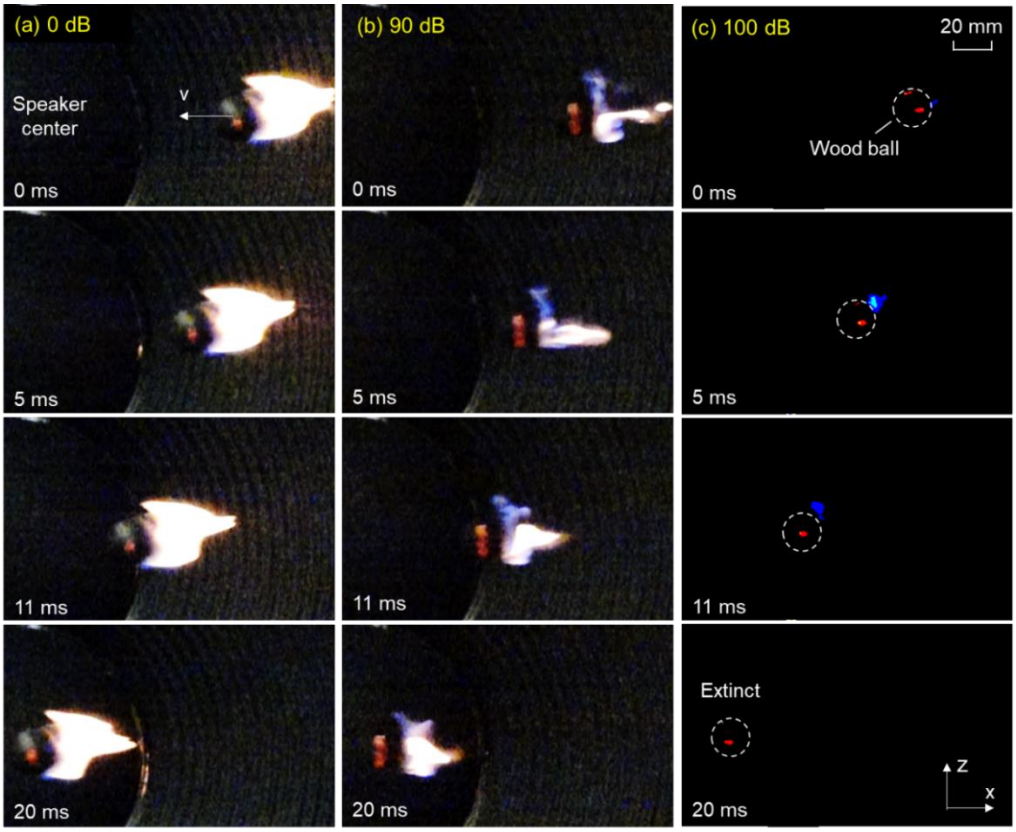

Fig. 7. High-speed images in front of the speaker at 960 fps for the fast-moving firebrands when θ = 60°. A 95-Hz acoustic field works with the pressures of (a) 0 dB (Video A3), (b) 90 dB (Video A4), and (c) 100 dB (Video A5), where images are sharpened to visualize the weak blue flame, and the time zero is the moment firebrand enters the main acoustic field.

Fig. 8 plots the critical acoustic extinction pressures versus the firebrand velocity at different frequencies. The most prominent feature here is that as the firebrand motion accelerates, a lower sound level is required to cause extinction. Also, increasing frequency has a noticeable impact on the growth in extinction pressure. Two factors, i.e., the firebrand motion and acoustic oscillation, should be responsible for triggering the extinction, so the coupling between two factors should be discussed.

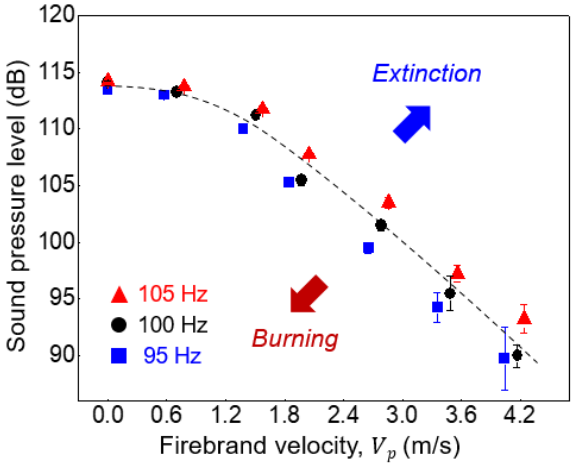

Fig. 8. The acoustic extinction pressure plotted as a function of firebrand instantaneous velocity at different frequencies, where the error bar shows the experimental random uncertainty.

3.3. Acoustic extinction mechanism

Usually, the extinction of wood flame can be explained by various mechanisms, like those based on the excessive weakening of thermal feedback or the minimum fuel mass loss rate [28, 29]. These existing theories, however, cannot directly address the sound-induced extinction. This work attempts to reach the physical impact of acoustic waves on firebrand extinction by borrowing the concept from the theory of stabilization of a lifted flame [30]. A model that describes the local behavior of flame on the firebrand prior to extinction from the x-y plane was formulated and presented in Fig. 9 (top view). Here, the target firebrand is moving within a sound field with an instantaneous velocity V_s, which is slightly lower than the peak swing velocity V_p. Behind the moving firebrand, a flame is attached and tilted by sounds waves. In between, there is a mixing of fuel gas and airflow within the wake region. The lifted flame leading edge is also a sign for premixing. For simplification, the fuel gas was assumed to be able to develop to a well-premixed mixture caused by the strong air recirculation behind a moving firebrand. In this way, the acoustic extinction of flame on a moving firebrand can be hypothesized as a failed ignition of the premixed fuel gas in the wake region.

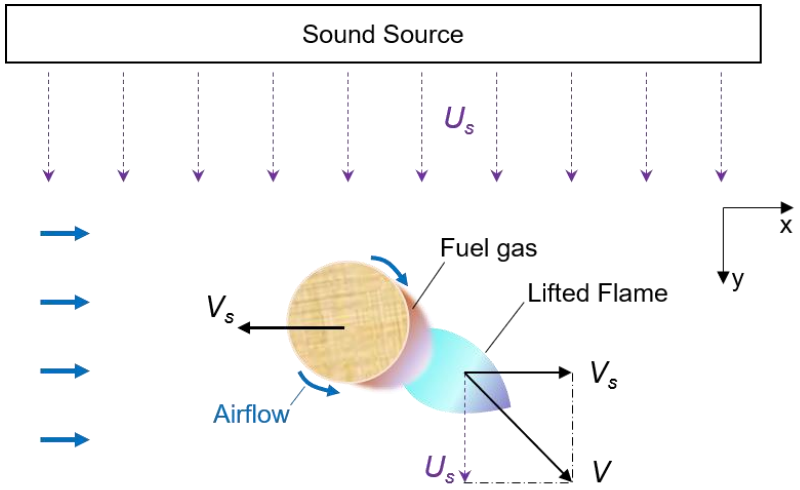

Fig. 9. A scientific illustration (top view) of acoustic extinction on the flame on a moving firebrand.

From the model above, a Damköhler number (Da) can be used to describe the ignitability of the fuel gas in the wake region [31], which also provides a bridge to connect flame with acoustic. A similar criterion Da^* for judging the flame extinction was formulated here, which is given by the ratio of the residence time (t_{re}) of fuel gas in the wake region to the pilot delay (t_{ig})

$$D_a^* = t_{re}/t_{ig} \tag{1}$$

For a successful pilot ignition, the fuel gas needs to mix with air first to reach the lower flammable limit and, subsequently, the mixture costs another moment for the gaseous chemical reaction to produce a flame. The former stage can be characterized by a mixing time (t_{mix}), and the latter can be characterized by a chemical time (t_{ch}). Eventually, the duration of the pilot delay is:

$$t_{ig} = t_{mix} + t_{ch} \tag{2}$$

Since the fuel gas in the wake region was assumed to be well premixed before being piloted, the mixing time can be ignored. This can be further evidenced by a theoretical estimation. Typically, there is a critical distance δ for the newly pyrolyzed fuel gas to mix with air and then develop to a premixed combustible gas. This can be calculated from $\delta = D/Nu_D$, where D = 20 mm is the characteristic length

that equals to the ball diameter. Due to the pendulum-induced fast motion, the Nusselt number (Nu_D) for the forced convection around a sphere [32] is used:

$$Nu_D = 2 + 0.6Re^{1/2}Pr^{1/3} \tag{3}$$

Here, Pr = 0.7 is the Prandtl number of air at 1300 K (the average of wood flame temperature and pyrolysis temperature), and $Re = V_s D/v$ is the Reynolds number. Eventually, Eq. (3) produces an average residing at Nu_D = 12.8, which leads to a critical premixed distance of δ = 1.56 mm. The video records, however, suggested that the gap (R) between the flame and firebrand approximates to 2 ± 0.5 mm prior to extinction (Fig. 7c), which means that the pyrolyzed gas can develop to a completely premixed one before being ignited. Thus, it is possible to take $t_{ig} = t_{ch}$ in this work.

The chemical time can be given by $t_{ch} = R/S_L$, where R denotes the gap width, and S_L is the laminar burning velocity, which has a typical value of 0.5 m/s [33]. As a result, the pilot delay is $t_{ig} = t_{ch} = 4$ ms. By re-examining Fig. 9, there are two factors that affect the residence time (t_{re}) of fuel gas to stay in the wake region: (1) the relative velocity V_s between the flame and ball, which equals the velocity of the firebrand. This is because in the coordinate of a moving firebrand the pyrolysis gas seems to be injected out from the burning piece, and (2) the sound-induced velocity U_s along the y-direction.

Since the target extinction only occurs within the uniform sound region, it can be considered that the critical pressure at a prescribed frequency, namely P_f^*, acts uniformly on the spherical surface. To introduce the sound-related parameters into the extinction criterion, an assumption was made in which the sound-induced velocity is replaced by $U_s = \sqrt{P_f^*/\rho}$, where $\rho = 0.26$ kg/m^3 is the air density at the average temperature of 1300 K. In this way, the critical sound pressure could be related to flame extinction, and the net velocity V that drives the premixed fuel gas out from the wake region is calculated as:

$$V = \sqrt{U_s^2 + V_s^2} = \sqrt{P_f^*/\rho + V_s^2} \tag{4}$$

A competition between the critical values of U_s and V_s is shown in Fig. 10a, where U_s is calculated by using the extinction pressure in Fig. 8, and V_s is obtained by measuring the high-speed video at the extinction position. Results indicated that the two types of velocity are of the same order, which confirms the combination of firebrand motion and acoustic wave as the primary factor that governs flame extinction.

Given that $t_{re} = D/V$, the original expression of Eq. (1) can be reformulated as

$$D_a^* = \frac{D/\sqrt{\left(P_f^*/\rho\right) + V_s^2}}{R/S_L} \tag{5}$$

Fig. 10b shows the solutions of Eq. (5) at the extinction limits. It was found that the application of this expression could yield consistent results that locate around 1.0. Further, this criterion shows an insensitivity in responding to frequency variation. Therefore, it can be defined as an effective indicator of acoustic conditions to separate the low-fire-hazard and high-fire-hazard regimes for a moving and flaming firebrand. Under the circumstance where $Da^* < 1.0$, the flaming firebrand can be extinguished due to the acoustic disruption of the wood-flame cycle. Otherwise, the flame should persist because of quick ignition.

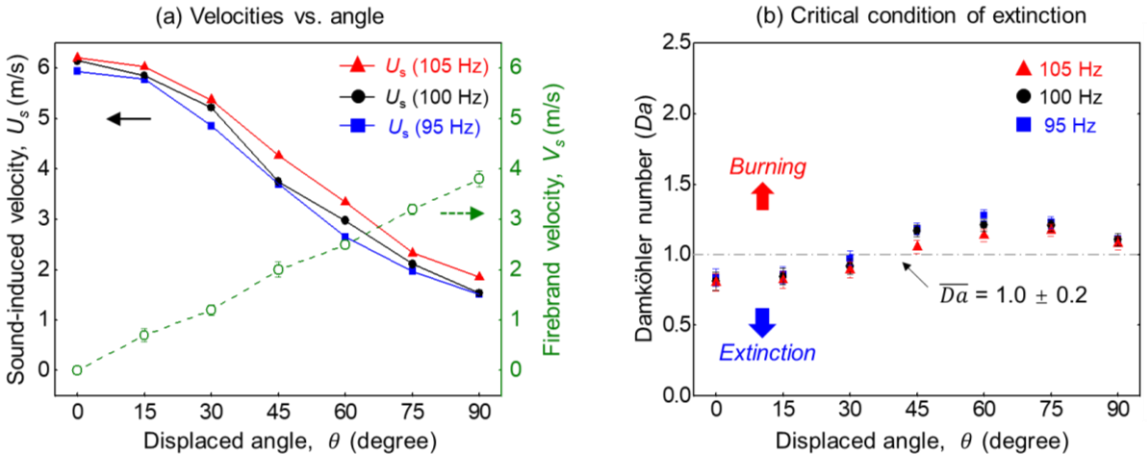

Fig. 10. (a) Comparison between sound-induced velocity (U_s) and firebrand velocity (V_s), and (b) the calculated values of Da^* at the extinction limit of different sound frequencies. The error bar denotes the measuring error by the decibel meter.

3.4. Fire technology applications

Based on the successful acoustic extinction of fast-moving flaming firebrands, a sound-based fire protection system can be designed for the residential houses in the WUI area to reduce the possibility of being remote-ignited by the large-density firebrand spotting. For instance, Fig. 11 illustrates an idealized acoustic WUI fire-protection system that shields the flaming firebrands. Here, multiple speakers were designed based on the house envelope to prevent the flaming firebrands from all directions. There is still a long way from the lab-scale research to real fire protection applications. Some key parameters require further investigations, such as the optimal incident angle of sound wave (e.g., the effective distance and perimeter) and its potential impact on human health. Nevertheless, this lab research has provided useful scientific insights into this application. For instance, the tested 20-mm firebrand sample is within the statistical range 18 ± 6 mm [27], and a maximum flying velocity 4.2 m/s allows the firebrand to transport for about 10 m [17, 25]. Because the flame of smaller firebrands has a lower HRR and is easier to extinguish, the critical acoustic field presented in this paper should be able to shield the flame of most real firebrands.

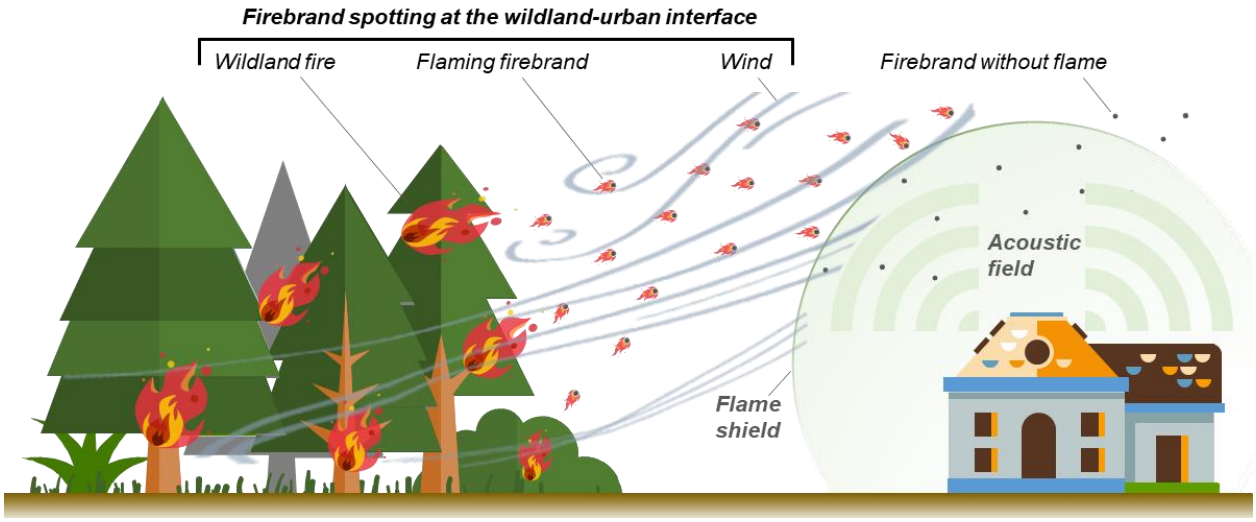

Fig. 11. Application of sound suppression technology to shield the flaming firebrands.

Compared with the conventional water- and gas-based fire suppression systems, this acoustic-based flame suppression system has some excellent advantages, because it is able to tackle the fast-moving flaming firebrand shower by generating a special shield for the house and community (see Fig. 1b). One possible limitation of this system is the high demand for the power of the speaker. Nevertheless, the intensity of the sound wave can be enhanced by guided reflection or producing the stationary waves, which requires a custom design of the acoustic field based on structure and landscape and should balance the firefighting performance and the overall cost.

On the other hand, smoldering or glowing firebrands with high temperature also significantly pose an ignition threat to WUI [34, 35], and their fire hazard could suddenly increase via the smoldering-to-flaming (StF) transition [23, 36]. In the experiment, we also found that the acoustic field increased the charring process on the sample surface while limiting the possibility of smoldering-to-flaming (StF) transition, because the flame fails to stabilize itself. To better understand of sound suppression on different WUI-fuels, more fundamental research on the effect of sound wave on firebrand size, chemistry, and moisture content are required. In addition, the impact of the sound wave on the smoldering firebrand is still unclear. To make the system more practical and reliable, an optimal design of the acoustic field, e.g., generating reflection waves and stationary waves, as well as saving energy, is required in future research.

4. Conclusions

This experimental work investigated the acoustical extinction of flame on moving firebrand. The characteristic firebrand was supported by the dry wood ball with a diameter of 20 mm and a mass of 2.9 g, and its motion was controlled by a pendulum system up to 4.2 m/s. The local sound pressure varied from 90 to 114.3 dB, and the sound frequency varied from 95 to 105 Hz. Results suggested a positive correlation between the sound pressure and frequency for extinguishing the firebrand flame.

Moreover, as the moving speed of firebrand increases from 0 to 4.2 m/s, the required minimum sound pressure for extinction decreases significantly from 114 dB to 90 dB. The cumulative effect of the firebrand motion and wave oscillation, which deflects the pyrolyzed fuel away from the firebrand, leads to a disruption of the fuel-flame cycle and invites extinction. A characteristic Damköhler number (1.0 ± 0.2) was found to characterize the ratio of the residence time of fuel to the chemical time of flame, which defines the critical sound condition for extinguishing a moving and flaming firebrand. The insights gained from the single flaming firebrand can aid the understanding of acoustic impact on the extinction of flame on the moving solid fuel. More complex acoustic-suppression configurations with multiple speakers and firebrand showers will be investigated in the larger-scale wind-tunnel tests and presented in the future work.

Acknowledgments

This study received financial support from National Natural Science Foundation of China (No. 52006185, 51876183), the National Key R&D Program of China (No. 2018YFB1501405), Hong Kong Polytechnic University (1-BE04), PolyU Emerging Frontier Area (EFA) Scheme of RISUD (P0013879), and ZJU SKLCEU Open Fund (ZJUCEU2018012).

References

1. O'Connor J, Acharya V, Lieuwen T (2015) Transverse combustion instabilities: Acoustic, fluid mechanic, and flame processes. Progress in Energy and Combustion Science 49:1–39 . doi: https://doi.org/10.1016/j.pecs.2015.01.001
2. Kim JS, Williams FA (1994) Contribution of strained diffusion flames to acoustic pressure

response. Combustion and Flame 98:279–299
3. Baillot F, Lespinasse F (2014) Response of a laminar premixed V-flame to a high-frequency transverse acoustic field. Combustion and Flame 161:1247–1267 . doi: 10.1016/j.combustflame.2013.11.009
4. Wang Q, Huang HW, Tang HJ, et al (2013) Nonlinear response of buoyant diffusion flame under acoustic excitation. Fuel 103:364–372 . doi: 10.1016/j.fuel.2012.08.008
5. DARPA Instant Flame Suppression Phase II - Final Report. The Defense Advanced Research Projects Agency 1–23
6. Friedman AN, Stoliarov SI (2017) Acoustic extinction of laminar line-flames. Fire Safety Journal 93:102–113 . doi: 10.1016/j.firesaf.2017.09.002
7. Niegodajew P, Łukasiak K, Radomiak H, et al (2018) Application of acoustic oscillations in quenching of gas burner flame. Combustion and Flame 194:245–249 . doi: 10.1016/j.combustflame.2018.05.007
8. Yamazaki T, Matsuoka T, Nakamura Y (2019) Dynamic Response of Non-premixed Flames subjected to Acoustic Wave. 12th Asia-Pacific Conference on Combustion, 4 Jul 2019
9. Xiong C, Liu Y, Xu C, Huang X (2020) Extinguishing the dripping flame by acoustic wave. Fire Safety Journal. doi: 10.1016/j.firesaf.2020.103109
10. Manzello SL, Suzuki S, Gollner MJ, Fernandez-Pello AC (2020) Role of firebrand combustion in large outdoor fire spread. Progress in Energy and Combustion Science 76:100801 . doi: 10.1016/j.pecs.2019.100801
11. Manzello SL (2014) Special Issue on Wildland-Urban Interface (WUI) Fires. Fire Technology 50:7–8
12. Manzello SL, Foote EID (2014) Characterizing Firebrand Exposure from Wildland-Urban Interface (WUI) Fires: Results from the 2007 Angora Fire. Fire Technology 50:105–124 . doi: 10.1007/s10694-012-0295-4
13. Pastor E (2003) Mathematical models and calculation systems for the study of wildland fire behaviour. Progress in Energy and Combustion Science 29:139–153 . doi: 10.1016/S0360-1285(03)00017-0
14. Koo E, Pagni PJ, Weise DR, Woycheese JP (2010) Firebrands and spotting ignition in large-scale fires. International Journal of Wildland Fire 19:818 . doi: 10.1071/WF07119
15. Caton SE, Hakes RSP, Gorham DJ, et al (2016) Review of Pathways for Building Fire Spread in the Wildland Urban Interface Part I: Exposure Conditions. Fire Technology 1–45 . doi: 10.1007/s10694-016-0589-z
16. Fernandez-Pello AC (2017) Wildland fire spot ignition by sparks and firebrands. Fire Safety Journal 91:2–10 . doi: 10.1016/j.firesaf.2017.04.040
17. Song J, Huang X, Liu N, et al (2017) The Wind Effect on the Transport and Burning of Firebrands. Fire Technology 53:1555–1568 . doi: 10.1007/s10694-017-0647-1
18. Manzello SL, Cleary TG, Shields JR, Yang JC (2006) Ignition of Vegetation and Mulch by Firebrands in Wildland/Urban Interface (WUI) Fires. Chemical and Physical Processes in Combustion 22 . doi: 10.1071/WF06031
19. Sardoy N, Consalvi JL, Porterie B, Fernandez-Pello AC (2007) Modeling transport and combustion of firebrands from burning trees. Combustion and Flame 150:151–169 . doi: 10.1016/j.combustflame.2007.04.008
20. Suzuki S, Manzello SL, Kagiya K, et al (2014) Ignition of Mulch Beds Exposed to Continuous Wind-Driven Firebrand Showers. Fire Technology. doi: 10.1007/s10694-014-0425-2
21. Manzello SL (2020) Introduction to the Special Section on Global Overview of Large Outdoor Fire Standards. Fire Technology. doi: 10.1007/s10694-020-00962-6
22. Tarifa CS, Notario PP Del, Moreno FG (1965) On the flight paths and lifetimes of burning particles of wood. Symposium (International) on Combustion 10:1021–1037 . doi: 10.1016/S0082-0784(65)80244-2
23. Santoso MA, Christensen EG, Yang J, Rein G (2019) Review of the Transition From Smouldering to Flaming Combustion in Wildfires. Frontiers in Mechanical Engineering 5: . doi: 10.3389/fmech.2019.00049
24. Suzuki S, Manzello SL (2018) Characteristics of Firebrands Collected from Actual Urban Fires. Fire Technology 54:1–14 . doi: 10.1007/s10694-018-0751-x

25. Filkov A, Prohanov S, Mueller E, et al (2017) Investigation of firebrand production during prescribed fires conducted in a pine forest. Proceedings of the Combustion Institute 36:3263–3270 . doi: 10.1016/j.proci.2016.06.125
26. Koo E, Linn RR, Pagni PJ, Edminster CB (2012) Modelling firebrand transport in wildfires using HIGRAD/FIRETEC. International Journal of Wildland Fire 21:396–417 . doi: 10.1071/WF09146
27. Manzello SL, Suzuki S (2017) Generating wind-driven firebrand showers characteristic of burning structures. Proceedings of the Combustion Institute 36:3247–3252 . doi: 10.1016/j.proci.2016.07.009
28. Bartlett AI, Hadden RM, Bisby LA (2019) A Review of Factors Affecting the Burning Behaviour of Wood for Application to Tall Timber Construction. Fire Technology 55:1–49 . doi: 10.1007/s10694-018-0787-y
29. Hadden RM, Law A (2020) The Variability of Critical Mass Loss Rate. Fire Technology. doi: 10.1007/s10694-020-01002-z
30. Science KL-P in E and C, 2007 undefined Toward an understanding of the stabilization mechanisms of lifted turbulent jet flames: experiments. Elsevier
31. Science FW-P in E and C, 2000 undefined Progress in knowledge of flamelet structure and extinction. Elsevier
32. Bergman T, Incropera F, Lavine A, DeWitt D (2011) Introduction to heat transfer. John Wiley & Sons, Inc., New York
33. Quintiere JG (1998) An introduction to fire dynamics
34. A M, B FJ, C KW (1976) Investigation of fire whirls and firebrands
35. Babrauskas V (2018) Firebrands and Embers. Encyclopedia of Wildfires and Wildland-Urban Interface (WUI) Fires 431–444 . doi: 10.1007/978-3-319-52090-2_3
36. Huang X, Gao J (2020) A review of near-limit opposed fire spread. Fire Safety Journal 103141 . doi: 10.1016/j.firesaf.2020.103141